

Plant Image Analysis

Fundamentals and Applications

Edited by
S. Dutta Gupta and Yasuomi Ibaraki



CRC Press

Taylor & Francis Group

Boca Raton London New York

CRC Press is an imprint of the
Taylor & Francis Group, an **informa** business

CRC Press
Taylor & Francis Group
6000 Broken Sound Parkway NW, Suite 300
Boca Raton, FL 33487-2742

© 2015 by Taylor & Francis Group, LLC
CRC Press is an imprint of Taylor & Francis Group, an Informa business

No claim to original U.S. Government works
Version Date: 20140717

International Standard Book Number-13: 978-1-4665-8302-3 (eBook - PDF)

This book contains information obtained from authentic and highly regarded sources. Reasonable efforts have been made to publish reliable data and information, but the author and publisher cannot assume responsibility for the validity of all materials or the consequences of their use. The authors and publishers have attempted to trace the copyright holders of all material reproduced in this publication and apologize to copyright holders if permission to publish in this form has not been obtained. If any copyright material has not been acknowledged please write and let us know so we may rectify in any future reprint.

Except as permitted under U.S. Copyright Law, no part of this book may be reprinted, reproduced, transmitted, or utilized in any form by any electronic, mechanical, or other means, now known or hereafter invented, including photocopying, microfilming, and recording, or in any information storage or retrieval system, without written permission from the publishers.

For permission to photocopy or use material electronically from this work, please access www.copyright.com (<http://www.copyright.com/>) or contact the Copyright Clearance Center, Inc. (CCC), 222 Rosewood Drive, Danvers, MA 01923, 978-750-8400. CCC is a not-for-profit organization that provides licenses and registration for a variety of users. For organizations that have been granted a photocopy license by the CCC, a separate system of payment has been arranged.

Trademark Notice: Product or corporate names may be trademarks or registered trademarks, and are used only for identification and explanation without intent to infringe.

Visit the Taylor & Francis Web site at
<http://www.taylorandfrancis.com>

and the CRC Press Web site at
<http://www.crcpress.com>

chapter eight

Thermal imaging for evaluation of seedling growth

Étienne Belin, David Rousseau, Landry Benoit, Didier Demilly, Sylvie Ducournau, François Chapeau-Blondeau, and Carolyne Dürr

Contents

8.1	Introduction.....	165
8.2	Experimental setup	166
8.3	Thermal imaging applied to seed imbibition.....	168
8.4	Thermal imaging applied to seed elongation.....	169
8.5	Conclusion	174
	Acknowledgments.....	175
	References.....	175

8.1 Introduction

Thermography is a noninvasive imaging method that gives access to temperature by use of the blackbody law. In the domain of plants, the measurement of the temperature is an important physical parameter. Additionally, apparent temperature provided by thermography is also indirectly related to other functional or structural parameters, like leaf orientation, heat capacity, surface properties, infrared (IR) absorption, and transpiration rate (Kana and Vass, 2008; Fiorani et al., 2012). Thermography has therefore been widely tested and shown useful on plants at various observation scales from canopy down to single leaf and in various biological contexts, including, for instance, evaluation of stomatal aperture (Leinonen et al., 2006), plant water content (Wang et al., 2010a, 2010b), plant freezing (Wisniewski et al., 2008), and the development of pathogens (Chaerle and der Staeten, 2001; Chaerle et al., 2007; Belin et al., 2013).

In this chapter, we work on the application of thermal imaging on seeds and seedlings (Dell'Aquila, 2009). The early stages of the development of the plant have only recently been analyzed with thermal imaging (Baranowski et al., 2003; Kranner et al., 2010; Belin et al., 2011). Thermal

imaging was first used to evaluate the germination capacity of legume seeds (Baranowski et al., 2003). The seed storage duration and the variations in germination speed were shown to induce significant thermal differences during the initial stage of the imbibition process. Biophysical and biochemical changes during imbibition and germination were also shown to be detectable with thermal imaging and useful to predict whether a quiescent seed will germinate or die upon water uptake (Kranter et al., 2010). Thermal imaging was shown useful to discriminate hypocotyl from radicle in *Medicago truncatula* during the elongation stage of the seedling (Belin et al., 2011). Because thermal imaging can be influenced by various parameters, it is necessary when working at a given observation scale to investigate the possible impact of the measuring environment on the information to be extracted from the scene. This was done, for instance, at the leaf scale in Kümmerlen et al. (1999). We propose to transpose such an approach when working with thermal imaging at the seed scale, and this chapter is organized as follows. Section 8.2 first describes the experimental setup used in this report for monitoring seed germination and elongation with thermography. In Sections 8.3 and 8.4, results are presented regarding the seed imbibition and seedling elongation stages with seeds of various species.

8.2 Experimental setup

Thermal imaging cameras are constituted, like in conventional imaging, with a lens that focuses infrared onto a detector (Breitenstein et al., 2003; Vollmer and Mollmann, 2010). The radiation that impinges on a thermal camera comes from three different sources. The camera receives radiation W_{obj} from the target object, plus radiation W_{amb} from its ambience that has been reflected onto the object surface. Both of these radiation components become attenuated when they pass through the atmosphere. Since the atmosphere absorbs part of the radiation, it will also radiate some itself, W_{atm} . The total radiation power received by the camera can therefore be expressed as

$$W_{tot} = \varepsilon\tau W_{obj} + (1 - \varepsilon)\tau W_{amb} + (1 - \tau)W_{atm}$$

where ε is the object emissivity and τ is the transmission through the atmosphere. In our experiment we have taken care to maintain at thermal equilibrium the environment surrounding the targeted seeds. The distance of observation was kept constant during the observation, at some tens of centimeters, to limit the absorption by the atmosphere and maximize the spatial resolution. As a result, the observed thermal contrasts are due to effective thermal contrasts in the seeds only. The emissivity for

seeds is not yet available in literature. The estimation of an emissivity is often done by placing a thermometer on the targeted object or by placing an adhesive rubber of known emissivity on part of the object. Given the size of the object observed here, the estimation of the emissivity has not been investigated. Emissivity was assumed constant and equal to unity in our experiment. We will discuss this assumption in the elongation phase later in the chapter. The majority of thermal imaging cameras have a microbolometer type detector, mainly because of cost considerations. Microbolometers generally do not require cooling, which allows compact camera designs that are relatively low in cost. Microbolometers operate in the wavelength window of 8 to 12 μm . The typical thermal resolution is 0.1°C . For more demanding applications in terms of thermal resolution (for instance, 0.01°C), quantum detectors are used. These quantum detectors require cooling systems and operate in the wavelength window of 2 to 5 μm . In the applications of thermal imaging presented here, observed thermal contrasts were between 0.01 and 0.1°C . An IR camera with a quantum detector was therefore used.

The resulting imaging setups used in this chapter are described in Figure 8.1. The setups differ for imbibition and elongation monitoring. Figure 8.1a describes the setup as used in Belin et al. (2011) for seedling elongation monitoring. The seedlings are placed in a system with regulated temperature and water content. The opening and closure of the system can be controlled and synchronized with the image acquisition of the thermal camera. Because of mechanical limitations the minimum time interval between two acquisitions is 2 min. This is not a limitation for

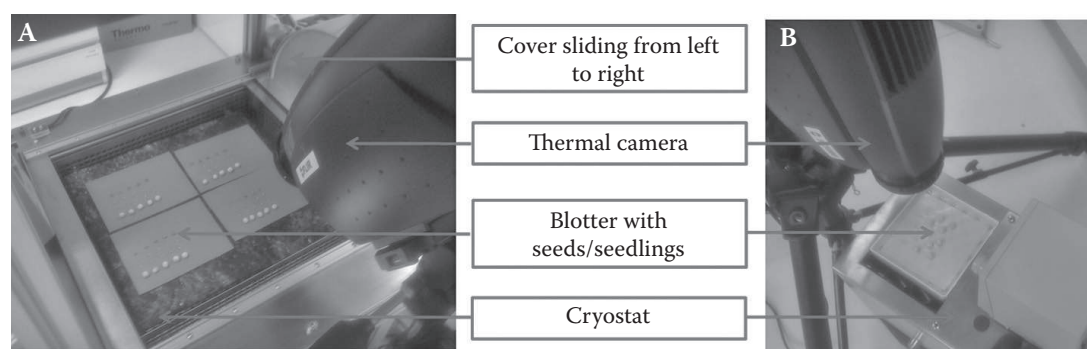


Figure 8.1 Thermal imaging computer vision system working in no-light conditions. Thermal images are acquired with a FLIR SC 5000 cooled infrared camera with a spectral range between 2.5 and 5 μm , a spatial resolution of 320×240 pixels, and a 12-bit dynamic. The thermal imager is positioned vertically above the seeds/seedlings. (a) Experimental setup for thermal imaging of seedlings during elongation phase. Seedlings are installed on blotter placed in a cryostat regulated at 20°C . (b) Experimental setup for thermal imaging of seeds' imbibition. Cryostat is regulated at 24°C . The entire system is placed in a growth chamber regulated at 24°C .

elongation monitoring, which is a biological process lasting several days. This is more limiting for the monitoring of imbibition, which is a faster biological process with important changes with time at hourly intervals. Figure 8.1b describes the setup used for seed imbibition and germination monitoring and reproducing the one introduced in Kranner et al. (2010).

8.3 Thermal imaging applied to seed imbibition

Thermal imaging was used to study seed imbibition and germination of different seeds species, such as the pea, oilseed rape, and wheat (Kranner et al., 2010). Seed imbibition is the very early stage essential for germination, and seed germination rates are dependent on imbibition rate. Seed imbibition was found to be associated with seed changes in temperature, detected in all the studied species, but with more or less large differences compared to dry seeds. This method would thus allow recording imbibition noninvasively. During the experiments carried out at 24°C, after a first and brief stage (<1 h) showing a temperature increase, a sharp temperature decrease was observed during 4–5 h, followed by a progressive reincrease in temperature. This temperature profile was more pronounced for the pea, with a drop in temperature of more than 1°C. It was also detectable, but limited to less than 0.1°C in wheat, and this drop was even lower in rape seeds. These changes in temperature were used to detect and predict nonviable seeds in the first 3 h of water uptake, a span of time that allows us to redry and store seeds after analysis without killing them. These typical temperature profiles measured for seeds were also compared for peas to a model of seed thermogenesis obtained using temperature calibration profiles measured for different soluble sugars and starch diluted at different concentrations. This approach indicated that the measured seed temperature profiles were coherent with biochemical changes and seed reserve transformation during germination. This opens roads for the use of infrared thermography to detect changes in seed and seedling metabolism noninvasively.

In the present report, as visible in [Figure 8.2](#), we have recorded non-monotonic temporal thermal evolution, as in Kranner et al. (2010), during the first hours following the beginning of the imbibition. This was obtained for pea seeds for which the thermal contrast was high, but we did not observe similar signatures with other species such as *M. truncatula* or sugar beet. We tried various techniques for seed imbibition, including Petri dishes on agar, sand, or blotter, like in Kranner et al. (2010). Such techniques are used for the monitoring with conventional RGB computer vision tools but did not allow recording of the short transitory period following the beginning of the imbibition. We therefore developed a setup similar to the one of Kranner et al. (2010) with polycarbonate plates, including multiple wells, each with an aperture at the bottom. When placed in a

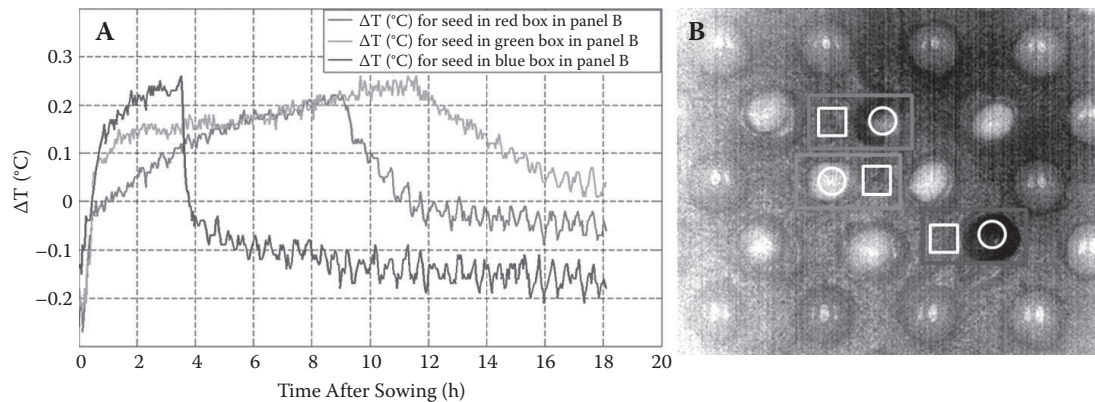


Figure 8.2 (See color insert.) Evolution of pea seeds' temperature during imbibition. (a) Evolution of the relative seed temperature ΔT after sowing for three different seeds. (b) Pea seeds sowed on a blotter. Studied seeds are identified with red, green, and blue boxes. Growth chamber, blotter, and water temperatures are fixed at 24°C. The relative seed temperature ΔT ($T_{seed} - T_{env}$) is defined as the difference between mean temperature T_{seed} of individual seed (white circles) and mean temperature of close environment T_{env} of seed (white squares).

water bath (temperature kept constant at 24°C, checked with a calibrated thermometer), the plates floated and the wells were constantly filled with water. The nonmonotonic thermal signature of Figure 8.2a is more pronounced, i.e., displays a larger variation of temperature, for higher temperature of the water and larger surface of contact between the water and the seed. This is made possible by maximizing the surface contact between the seeds and the water supply.

8.4 Thermal imaging applied to seed elongation

Seedling elongation is an early stage of the development of plants. During this stage, the seed is in the soil. Following a geotropism, the seedling shoot grows to reach the light and activates photosynthesis, while the lower part of the seedling, the radicle, goes deeper, anchors in the soil, and gives larger access to water and nutrients. The rates of elongation depend on environmental conditions, and also on species and genotype. Phenotyping the genetic diversity of these plant parameters could help breeding for improved plant tolerance to environmental stresses. In addition, differences in early radicle growth rates may be predictive of differences in adult plant root growth, which are much more difficult to measure. These plant parameters have also been used in plant growth models that predict emergence and crop growth. Finally, more deterministic molecular studies on plant growth use hypocotyls as model plant parts for which different mutants are available and which need to be phenotyped (Fankhauser and Staiger, 2002; Nagy and Schafer, 2002). Computer vision tools therefore stand as interesting solutions to monitor seedling

elongation. There exist a variety of approaches using conventional imaging with light in the visible spectrum (Kimura and Yamasaki, 2003; Basu et al., 2007; Armengaud et al., 2009; French et al., 2009; Wang et al., 2009; Yazdanbakhsh and Fisahn, 2010; Naeem et al., 2011; Cole et al., 2011). One limit of these computer vision tools is the use of light for image acquisition. The seedling grows in the soil in the absence of light. If exposed to visible light, its upper part stops elongating because of the seedling light receptors and new leaves expand. The study of seedling heterotrophic growth thus requires mimicking dark conditions. This is afforded by thermal imaging, which operates with infrared radiation and no need of visible light. Belin et al. (2011) illustrated the possibility of transposing the computer vision tool developed for seedling growth with visible imaging to the domain of infrared thermal imaging. This is possible because the thermal contrast between the seedling and the background is strong enough (typically 0.3°C). An additional contrast was also shown in thermal images, as a thermal discontinuity was visible along the seedlings themselves. The location of this thermal discontinuity is precisely lying at the frontier between the radicle and the hypocotyl. The hypocotyl part is hotter than the radicle part with an average difference of 0.5°C .

Before pushing further the investigation of thermal imaging applied to seedling elongation, we first consider the impact of environmental parameters on the thermal discontinuity. The imaging system of Figure 8.1a is equipped with an opening of the sliding cover synchronized with image acquisition. The opening of the cover is likely to bring convection. It is therefore important to control the impact of the opening of the cover on the thermal contrast observed on the seedlings. The entire process of cover opening (open, then remain open, then close) lasts in our experiment for 120 s. To study the influence of this opening in terms of thermal exchanges, we have made a continuous recording during the 120 s of the opening of the cover. The results are presented in Figures 8.3 and 8.4. As visible in Figure 8.3, the temperature of the blotter slowly decreases during cover opening. The variation is around 0.2°C between the beginning and end. During cover opening, temperatures for seedlings almost remain constant, taking into account standard deviation. Concerning the thermal discontinuity along the seedlings themselves, as visible in Figure 8.4 for three *M. truncatula* seedlings, despite some thermal variations, the difference of temperature ($T_{hyp} - T_{rad}$) remains positive during the 120 s. This shows that the thermal discontinuity (with the hypocotyl part hotter than the radicle part) between seedling parts is well preserved during all the duration of cover opening of 120 s used in our procedure.

Another question is the impact of lightening on the thermal discontinuity. It is possible to work with the imaging system of Figure 8.1a in dark conditions or to add light. Photoreceptors influencing germination and seedling growth are sensitive in blue and red/far-red wavelengths (Smith,

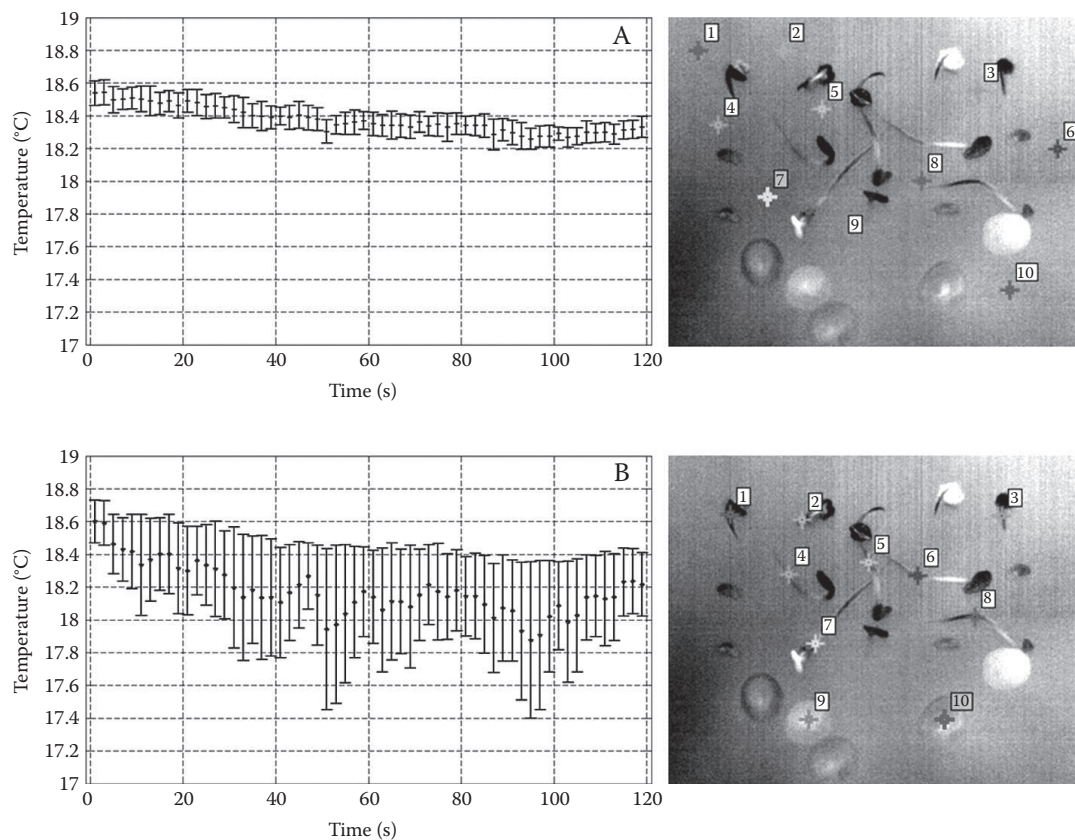


Figure 8.3 Thermal impact of cover opening. (a) Mean evolution (\pm standard deviation) of temperature of blotter during cover opening (duration: 120 s). Measurements are done in 10 different locations (color crosses on right image) on the blotter. (b) Mean evolution (\pm standard deviation) of temperature of seedling during cover opening (duration: 120 s). Measurements are done in 10 different locations (color crosses on right image) on seedlings (cotyledons, root system).

2000). One can wonder if the light has an influence on the thermal discontinuity observed. As visible in [Figure 8.5](#) and [Table 8.1](#), the thermal discontinuities are of the same order of magnitude in the presence of white light-emitting diode (LED) and in dark conditions. We observe no impact of such LED light on the thermal discontinuity. However, light will impact the elongation speed, and it is interesting to note that thermal imaging operating in dark and light conditions would be a potential tool to study the influence of light on seedling elongation.

Having estimated the absence of impact of environmental parameters on the thermal contrasts we measured, we push forward our investigation on the interest of thermal imaging for seedling elongation monitoring on seedlings from other species with the same procedure used for *M. truncatula* (Belin et al., 2011). Seedlings of nine different species have been placed under the imaging system of [Figure 8.1a](#). In [Figure 8.6](#), a thermal difference is visible between the seedlings and the background and along the seedlings themselves. The thermal discontinuity along the seedlings

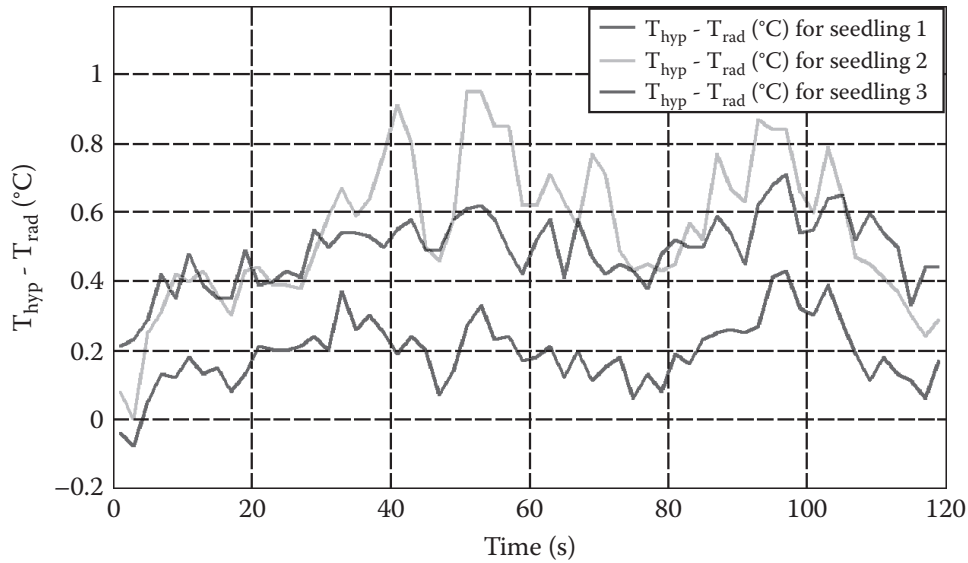


Figure 8.4 Time evolution of the difference of temperature ($T_{hyp} - T_{rad}$) between seedling organs (radicle and hypocotyl) during cover opening for three different seedlings of *M. truncatula*.

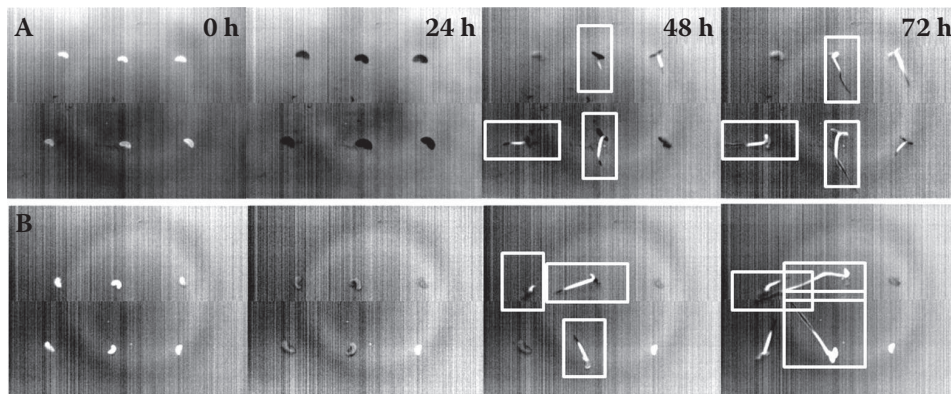


Figure 8.5 Influence of light on organs' temperature during elongation of seedlings of *M. truncatula*. Seedlings are illuminated in white light LED (a) during 1 min every 15 min, starting after sowing (0 h) and ending 3 days after (72 h). (b) Reference, as seedlings are kept in dark conditions for the entire duration of the experiment. The study of light influence on organ temperatures is taken at two measurements (48 h and 72 h), and it takes into account an average result of three seedlings (white boxes) per condition. Measurement points on seedlings are chosen manually in areas where contrasts are easily visible.

Table 8.1 Mean Value of the Difference of Temperatures ($T_{hyp} - T_{rad}$) between Organs (Hypocotyl and Radicle) Taken into Account for Three Seedlings and Two Conditions as Described in Figure 8.5

	White light	Dark conditions
Mean value of the difference of temperature at 48 h (°C)	0.900	0.945
Mean value of the difference of temperature at 72 h (°C)	0.896	0.662

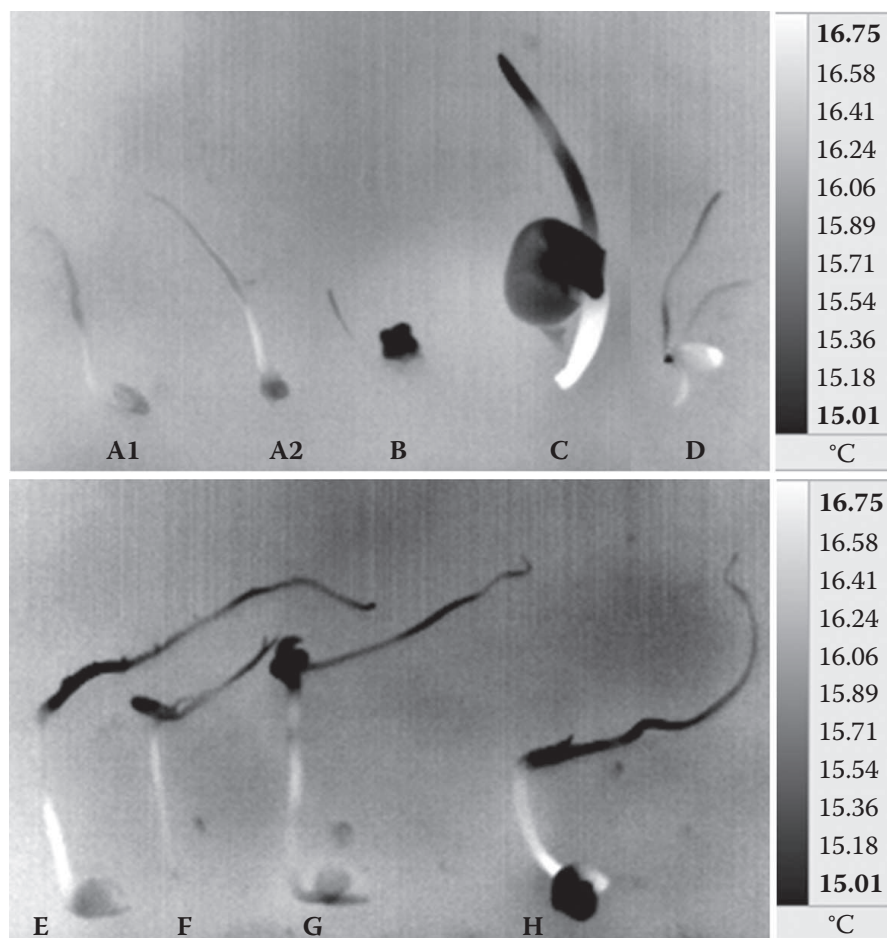


Figure 8.6 Thermal images of seedlings of various species during elongation phase. Seedlings are positioned with the entire root system (radicle + hypocotyl) in physical contact with the wet blotter. Seedlings are placed on the wet blotter 2 h before image acquisition, so that observed contrasts cannot be related to the thermal changing of the seedlings' environment. A1, *M. truncatula* (genotype A17); A2, *M. truncatula* (genotype F83); B, sugar beet; C, pea; D, wheat; E, mustard; F, ray grass; G, turnip rape; H, radish.

is located at the frontier between the radicle and the hypocotyl just as observed with *Medicago*. Illustrations of Figure 8.6 demonstrate the robustness and genericity of the presence of a thermal discontinuity observed between seedling parts of various species.

A first interpretation of the origin of this thermal discontinuity is based on functional hypotheses. During seedling heterotrophic growth, large fluxes of metabolites move from the storage organs to the elongating zones. The elongating radicle receives metabolites from seed reserve hydrolysis, and absorbs water and minerals from the growth support, as well as the seedling upper part growing toward the soil surface. Osmolyte molecules, like soluble sugars, are stored in the large cell vacuoles (Elamrani et al., 1992; Verscht, 2006). Contrasts in seedling parts in thermal images could therefore be due to such differences in fluxes and composition. Measurements of thermal discontinuities proved to be efficient for investigating sap streams on adult plants (Weibel and de Vos, 1994). Such contrasts obtained by heating a specific point in a plant part and linked to plant metabolism could be investigated in seedlings. It would be interesting to analyze how the amplitude of the thermal contrast during elongation is correlated with the chemical content of the seedling parts to investigate the validity of this functional hypothesis. The thermal contrasts observed for the nine species, varying from around 0.1°C for the lowest contrasts to around 0.5°C for the highest contrasts, may be correlated with differences in seedling biochemical compositions according to species.

Another complementary interpretation to account for the thermal contrast observed between the radicle and the hypocotyl is more anatomical. The epiderm of the radicle develops specifically long cells corresponding to very small root hairs, increasing the surface of exchange enabling the absorption of water. These long cells, measuring up to 100 microns, do not exist in the hypocotyl part. In addition to increasing the absorbing surface of the radicle, the absorbing cells change the roughness of the surface of the radicle. This could constitute a change of the emissivity, decreasing the perceived radiation from the radicle. It would be interesting to test if the thermal contrast still exists when monitoring the elongation of mutants that do not contain these long absorbing cells. Such experiments to interpret the thermal contrast observed during elongation of seedlings could be interesting to constitute thermal contrast as a new potential phenotypic trait to discriminate between different populations in a nondestructive and noninvasive way.

8.5 Conclusion

In this chapter, we have presented thermal imaging as a performance tool for the monitoring of seedling development, including germination

and elongation phases. During imbibition, thermal imaging can predict whether a quiescent seed is dead or will germinate upon water uptake (Kranner et al., 2010). During elongation, thermal imaging serves to distinguish between radicle and hypocotyl (Belin et al., 2011). We have demonstrated the reproducibility of these recent results, especially by investigating the impact of environmental parameters and of the experimental setup. We have also demonstrated that similar thermal discontinuities are also observable with other seed species. The physiological interpretation of the observed thermal discontinuity is still open for further investigations.

Acknowledgments

Landry Benoit acknowledges financial support for the preparation of his PhD from Angers Loire Métropole and GEVES-SNES. This work received support from the French government supervised by the Agence Nationale de la Recherche in the framework of the program Investissements d'Avenir under reference ANR-11-BTBR-0007.

References

- Armengaud, P., Zambaux, K., Hills, A., Sulpice, R., Pattison, R., Blatt, M., and Antmann, A., Ez-rhizo: integrated software for the fast and accurate measurement of root system architecture, *Plant J.*, 57, 945–956, 2009.
- Baranowski, P., Mazurek, W., and Walczak, R.T., The use of thermography for pre-sowing evaluation of seed germination capacity, in *Proceedings of the International Conference on Quality Chains: An Integrated View on Fruit and Vegetable Quality*, Wageningen, Netherlands, 2003, vols. 1 and 2.
- Basu, P., Pal, A., Lynch, J., and Brown, K., A novel image-analysis technique for kinematic study of growth and curvature, *Plant Physiol.*, 145, 305–316, 2007.
- Belin, E., Rousseau, D., Boureau, T., and Caffier, V., Thermography versus chlorophyll fluorescence imaging for detection and quantification of apple scab, *Comput. Electron. Agric.*, 90, 159–163, 2013.
- Belin, E., Rousseau, D., Rojas-Varela, J., Demilly, D., Wagner, M.H., Cathala, M.H., and Durr, C., Thermography as a non-invasive imaging for monitoring seedling growth, *Comput. Electron. Agric.*, 79, 236–240, 2011.
- Breitenstein, O., Warta, W., and Langenkamp, M., *Lock-in thermography*, Springer, New York, 2003.
- Chaerle, L., Leinonen, I., Jones, H.G., and der Straeten, D.V., Monitoring and screening plant populations with combined thermal and chlorophyll fluorescence imaging, *J. Exp. Bot.*, 58, 773–784, 2007.
- Chaerle, L., and der Straeten, D.V., Seeing is believing: imaging techniques to monitor plant health, *Biochim. Biophys. Acta*, 1519, 153–166, 2001.
- Cole, B., Kay, S.A., and Chory, J., Automated analysis of hypocotyl growth dynamics during shade avoidance in *Arabidopsis*, *Plant J.*, 65, 991–1000, 2011.
- Dell'Aquila, A., Development of novel techniques in conditioning, testing and sorting seed physiological quality, *Seed Sci. Technol.*, 37, 608–624, 2009.

- Elamrani, A., Gaudillere, J.P., and Raymond, P., Nature and utilization of seed reserves during germination and heterotrophic growth of young sugar beet seedlings, *Seed Sci. Res.*, 2, 1–8, 1992.
- Fankhauser, C., and Staiger, D., Photoreceptors in *Arabidopsis thaliana*: light perception, signal transduction and entrainment of the endogenous clock, *Planta*, 216, 1–16, 2002.
- Fiorani, F., Rascher, U., Jahnke, S., and Schurr, U., Imaging plants dynamics in heterogenic environments, *Curr. Opin. Biotechnol.*, 23, 227, 2012.
- French, A., Ubeda-Thomas, S., Holman, T.J., Bennett, M.J., and Pridmore, T., High-throughput quantification of root growth using a novel image-analysis tool, *Plant Physiol.*, 150, 1784–1795, 2009.
- Kana, R., and Vass, I., Thermo-imaging as a tool for studying light-induced heating of leaves correlation of heat dissipation with the efficiency of photosystem II photochemistry and non-photochemical quenching, *Environ. Exp. Bot.*, 57, 90–96, 2008.
- Kimura, K., and Yamasaki, S., Accurate root length and diameter measurement using NIH image: use of Pythagorean distance for diameter estimation, *Plant Soil*, 254, 305–315, 2003.
- Kranner, I., Kastberger, G., Hartbauer, M., and Pritchard, H.W., Non-invasive diagnosis of seed viability using infrared thermography, *Proc. Natl. Acad. Sci. USA*, 107, 3912–3917, 2010.
- Kümmerlen, B., Dauwe, S., Schmundt, D., and Schurr, U., Thermography to measure water relations of plant leaves, in *Handbook of computer vision and applications 3*, ed. B. Jähne, H. Haussecker, and P. Geissler, 763–781, Academic Press, Boston, 1999.
- Leinonen, I., Grant, O.M., Tagliavia, C.P.P., Chaves, M.M., and Jones, H.G., Estimating stomatal conductance with thermal imagery, *Plant Cell Environ.*, 29, 1508–1518, 2006.
- Naeem, A., French, A., Wells, D., and Pridmore, T., High-throughput feature counting and measurement of roots, *Bioinformatics*, 27, 1337–1338, 2011.
- Nagy, F., and Schafer, E., Phytochromes control photomorphogenesis by differentially regulated, interaction signaling pathways in higher plants, *Annu. Rev. Plant Biol.*, 53, 329–355, 2002.
- Smith, H., Phytochromes and light signal by plants—an emerging synthesis, *Nature*, 407, 585–591, 2000.
- Verscht, J., Sugar concentrations along and across the *Ricinus communis* L. hypocotyls measured by single cell sampling analysis, *Planta*, 224, 1303–1317, 2006.
- Vollmer, M., and Mollmann, K., *Infrared thermal imaging: fundamentals, research and applications*, Wiley, Weinheim, 2010.
- Wang, L., Uilecan, I.V., Assadi, A.H., Kozmik, C.A., and Spalding, E.P., Hypotrace: image analysis software for measuring hypocotyl growth and shape demonstrated on *Arabidopsis* seedlings undergoing photomorphogenesis, *Plant Physiol.*, 149, 1632–1637, 2009.
- Wang, X.Z., Yang, W.P., Wheaton, A., Cooley, N., and Moran, B., Automated canopy temperature estimation via infrared thermography: a first step towards automated plant water stress monitoring, *Comput. Electron. Agric.*, 73, 74–83, 2010a.
- Wang, X.Z., Yang, W.P., Wheaton, A., Cooley, N., and Moran, B., Efficient registration of optical and IR images for automatic plant water stress assessment, *Comput. Electron. Agric.*, 74, 230–237, 2010b.

- Weibel, F.P., and de Vos, J.A., Transpiration measurements on apple trees with an improved stem heat balance method, *Plant Soil*, 166, 203–209, 1994.
- Wisniewski, M., Glenn, D.M., Gusta, L., and Fuller, M.P., Using infrared thermography to study freezing in plants, *HortScience*, 43, 1648–1651, 2008.
- Yazdanbakhsh, N., and Fisahn, J., Analysis of *Arabidopsis thaliana* root growth kinetics with high temporal and spatial resolution, *Ann. Bot.*, 105, 783–791, 2010.

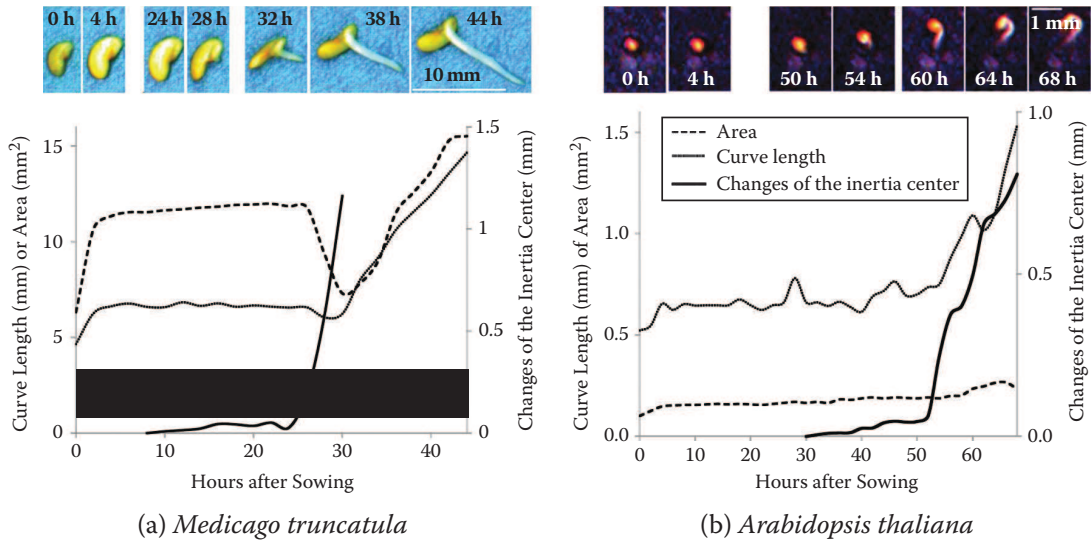


Figure 7.5 Sequence of images and main image analysis parameters extracted from sowing to radicle elongation stages of germination for (a) *M. truncatula* and (b) *A. thaliana*.

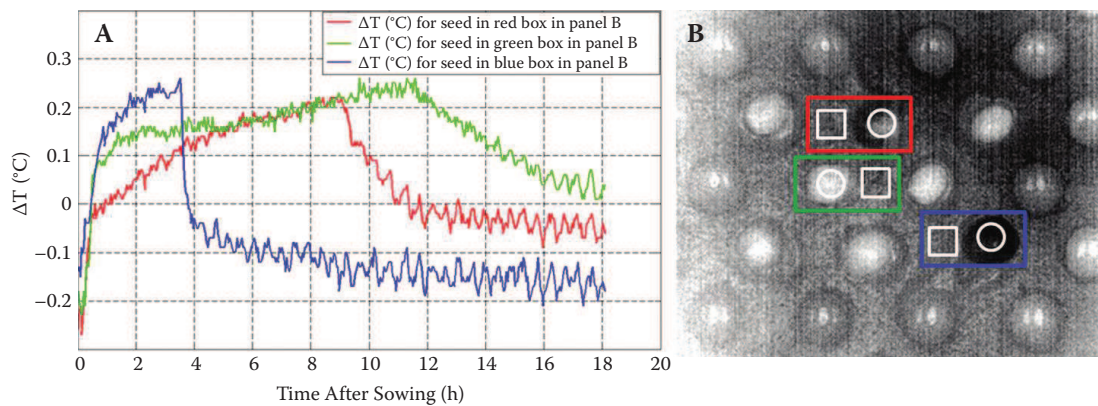


Figure 8.2 Evolution of pea seeds' temperature during imbibition. (a) Evolution of the relative seed temperature ϵT after sowing for three different seeds. (b) Pea seeds sowed on a blotter. Studied seeds are identified with red, green, and blue boxes. Growth chamber, blotter, and water temperatures are fixed at 24°C. The relative seed temperature ϵT ($T_{seed} - T_{env.}$) is defined as the difference between mean temperature T_{seed} of individual seed (white circles) and mean temperature of close environment $T_{env.}$ of seed (white squares).